

# Light-cone-like spreading of correlations in a quantum many-body system

Marc Cheneau<sup>1</sup>, Peter Barmettler<sup>2</sup>, Dario Poletti<sup>2</sup>, Manuel Endres<sup>1</sup>, Peter Schauß<sup>1</sup>, Takeshi Fukuhara<sup>1</sup>, Christian Gross<sup>1</sup>, Immanuel Bloch<sup>1,3</sup>, Corinna Kollath<sup>2,4</sup> & Stefan Kuhr<sup>1,5</sup>

In relativistic quantum field theory, information propagation is bounded by the speed of light. No such limit exists in the non-relativistic case, although in real physical systems, short-range interactions may be expected to restrict the propagation of information to finite velocities. The question of how fast correlations can spread in quantum many-body systems has been long studied<sup>1</sup>. The existence of a maximal velocity, known as the Lieb–Robinson bound, has been shown theoretically to exist in several interacting many-body systems (for example, spins on a lattice<sup>2–5</sup>)—such systems can be regarded as exhibiting an effective light cone that bounds the propagation speed of correlations. The existence of such a ‘speed of light’ has profound implications for condensed matter physics and quantum information, but has not been observed experimentally. Here we report the time-resolved detection of propagating correlations in an interacting quantum many-body system. By quenching a one-dimensional quantum gas in an optical lattice, we reveal how quasiparticle pairs transport correlations with a finite velocity across the system, resulting in an effective light cone for the quantum dynamics. Our results open perspectives for understanding the relaxation of closed quantum systems far from equilibrium<sup>6</sup>, and for engineering the efficient quantum channels necessary for fast quantum computations<sup>7</sup>.

Lieb–Robinson bounds have already found a number of fundamental applications<sup>8,9</sup>. For example, they enable a rigorous proof of a long-standing conjecture that linked the presence of a spectral gap in a lattice system to the exponential decay of correlations in the ground state<sup>10,11</sup>. They also provide fundamental scaling laws for entanglement entropy, which is an indicator of the computational cost of simulating strongly interacting systems<sup>12</sup>. Despite intensive theoretical work, the extent to which Lieb–Robinson bounds for interacting spins on a lattice<sup>2–5</sup> can be generalized remains however an open question<sup>13–16</sup>.

In the context of quantum many-body systems, the existence of a Lieb–Robinson bound can be probed by recording the dynamics following a sudden parameter change (a quench) in the Hamiltonian. In that case, a simple picture has been suggested: quantum-entangled quasiparticle pairs emerge from the initially highly excited state and propagate ballistically<sup>3</sup>, carrying correlations across the system. Ultracold atomic gases offer an ideal test bed for exploring such quantum dynamics owing to their almost perfect decoupling from the environment and their fast tunability<sup>17</sup>. In addition, the recently demonstrated technique of single-site imaging in an optical lattice<sup>18,19</sup> offers the resolution and sensitivity necessary to reveal the dynamical evolution of a many-body system at the single-particle level.

Our system consists of ultracold bosonic atoms in an optical lattice and is well described by the Bose–Hubbard model<sup>20,21</sup>. This model is parameterized by two energy scales: the on-site interaction,  $U$ , and the tunnel coupling between adjacent sites,  $J$ . Driven by the competition of these two parameters, a quantum phase transition between a superfluid and a Mott-insulating phase occurs in homogeneous systems where each lattice site is filled by an integer number of atoms,  $\bar{n}$ . In

the one-dimensional geometry considered here, the critical point of this transition is located at  $(U/J)_c \approx 3.4$  (ref. 22). We observed the time evolution of spatial correlations after a fast decrease of the effective interaction strength  $U/J$ , from an initial value deep in the Mott-insulating regime, with filling  $\bar{n} = 1$ , to a final value closer to the critical point (Fig. 1a). After such a quench, the initial many-body state  $|\Psi_0\rangle$  is highly excited and acts as a source of quasiparticles. In order to elucidate the nature and the dynamics of these quasiparticles, we have developed an analytical model in which the occupancy of each lattice site is restricted to  $n = 0, 1$  or 2 (Supplementary Information). For large interaction strengths, the quasiparticles consist of either an excess particle (‘doublon’) or a hole (‘holon’) on top of the unity-filling background. The quasiparticles inherit the bosonic nature of the atoms, but they can be turned into fermions (fermionized) using a Jordan–Wigner transformation. This allows us to partially eliminate the non-physical states in which a lattice site would be occupied by two quasiparticles. To first order in  $J/U$ , we then find that the many-body state at time  $t$  after the quench reads:

$$|\psi(t)\rangle \approx |\psi_0\rangle + i\sqrt{8}\frac{J}{U} \sum_k \sin(ka_{\text{lat}}) \left[ 1 - e^{-i[\varepsilon_d(k) + \varepsilon_h(-k)]t/\hbar} \right] \hat{a}_k^\dagger \hat{h}_{-k}^\dagger |\psi_0\rangle \quad (1)$$

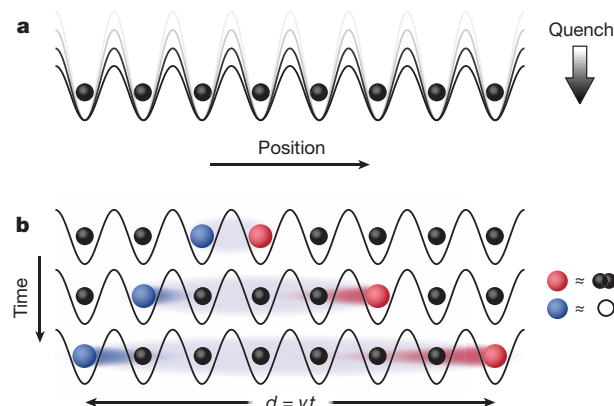


**Figure 1 | Spreading of correlations in a quenched atomic Mott insulator.** **a**, A one-dimensional ultracold gas of bosonic atoms (black balls) in an optical lattice is initially prepared deep in the Mott-insulating phase with unity filling. The lattice depth is then abruptly lowered (arrow at right), bringing the system out of equilibrium. **b**, Following the quench, entangled quasiparticle pairs emerge at all sites. Each of these pairs consists of a doublon and a holon (red and blue ball, respectively; see key at right) on top of the unity-filling background that propagate ballistically in opposite directions. It follows that a correlation in the parity of the site occupancy builds up at time  $t$  between any pair of sites separated by a distance  $d = vt$ , where  $v$  is the relative velocity of the doublons and holons.

<sup>1</sup>Max-Planck-Institut für Quantenoptik, 85748 Garching, Germany. <sup>2</sup>Département de physique théorique, Université de Genève, 1211 Genève, Switzerland. <sup>3</sup>Ludwig-Maximilians-Universität, 80799 München, Germany. <sup>4</sup>Centre de physique théorique, École Polytechnique, CNRS, 91128 Palaiseau, France. <sup>5</sup>University of Strathclyde, SUPA, Glasgow G4 0NG, UK.

The operators  $\hat{d}_k^\dagger$  and  $\hat{h}_{-k}^\dagger$  create a doublon with momentum  $k$  and energy  $\varepsilon_d(k)$ , and a holon with momentum  $-k$  and energy  $\varepsilon_h(-k)$ , respectively.  $k$  belongs to the first Brillouin zone and  $a_{\text{lat}}$  is the lattice period. Quasiparticles thus emerge at any site in the form of entangled pairs, consisting of a doublon and a holon with opposite momenta. Some of these pairs are bound on nearest-neighbour sites while the others form wave packets, owing to their peaked momentum distribution. The wave packets propagate in opposite directions with a relative group velocity  $v$  determined by the dispersion relation  $\varepsilon_d(k) + \varepsilon_h(-k)$  (Fig. 1b). The propagation of quasiparticle pairs is reflected in the two-point parity correlation functions<sup>23</sup>:

$$C_d(t) = \langle \hat{s}_j(t) \hat{s}_{j+d}(t) \rangle - \langle \hat{s}_j(t) \rangle \langle \hat{s}_{j+d}(t) \rangle \quad (2)$$

where  $j$  generally labels the lattice sites and  $d$  denotes the distance between the two sites considered. The operator  $\hat{s}_j(t) = e^{i\pi[\hat{n}_j(t) - \bar{n}]}$  measures the parity of the occupation number  $\hat{n}_j(t)$ . It yields  $+1$  in the absence of quasiparticles (odd occupancy) and  $-1$  if a quasiparticle is present (even occupancy). Because the initial state is close to a Fock state with one atom per lattice site, we expect  $C_d(t=0) \approx 0$ . After the quench, the propagation of quasiparticle pairs with relative velocity  $v$  results in a positive correlation between any pair of sites separated by a distance  $d = vt$ .

The experimental sequence started with the preparation of a two-dimensional degenerate gas of  $^{87}\text{Rb}$  confined in a single antinode of a vertical optical lattice<sup>19,23</sup> ( $z$  axis,  $a_{\text{lat}} = 532$  nm). The system was then divided into about 10 decoupled one-dimensional chains by adding a second optical lattice along the  $y$  axis and by setting both lattice depths to  $20.0(5) E_r$  (the number in parenthesis denotes the uncertainty of the last digit; see Methods), where  $E_r = (2\pi\hbar)^2 / (8ma_{\text{lat}}^2)$  is the recoil energy of the lattice and  $m$  the atomic mass of  $^{87}\text{Rb}$ . The effective interaction strength along the chains was tuned via a third optical lattice along the  $x$  axis. The number of atoms per chain ranged between 10 and 18, resulting in a lattice filling  $\bar{n} = 1$  in the Mott-insulating domain. The initial state was prepared by adiabatically increasing the  $x$ -lattice depth until the interaction strength reached a value of  $(U/J)_0 = 40(2)$ . At this point, we measured the temperature to be  $T \approx 0.1 U/k_B$  ( $k_B$  is the Boltzmann constant) following the method described in ref. 19. We then brought the system out of equilibrium by lowering the lattice depth, typically within  $100 \mu\text{s}$ , which is fast compared to the inverse tunnel coupling  $\hbar/J$ , but still adiabatic with respect to transitions to higher Bloch bands. The final lattice depths were in the Mott-insulating regime, close to the critical point. After a variable evolution time, we ‘froze’ the density distribution of the many-body state by rapidly raising the lattice depth in all directions to  $\sim 80 E_r$ . Finally, the atoms were detected by fluorescence imaging using a microscope objective with a resolution of the order of the lattice spacing and a reconstruction algorithm extracted the occupation number at each lattice site<sup>19</sup>. Because inelastic light-assisted collisions during the imaging led to a rapid loss of atom pairs, we directly detected the parity of the occupation number.

Our experimental results for the time evolution of the two-point parity correlations after a quench to  $U/J = 9.0(3)$  show a clear positive signal propagating with increasing time to larger distances  $d$  (Fig. 2). In addition, the propagation velocity of the correlation signal is constant over the range  $2 \leq d \leq 6$  (Fig. 2 inset), demonstrating that the correlations spread along an effective light cone. We also found similar dynamics for quenches to  $U/J = 5.0(2)$  and  $7.0(3)$  (Supplementary Fig. 1). We note that the observed signal cannot be attributed to a simple density wave because such an excitation would result in  $\langle \hat{s}_j \hat{s}_{j+d} \rangle = \langle \hat{s}_j \rangle \langle \hat{s}_{j+d} \rangle$ . We compared the experimental results to numerical simulations of an infinite, homogeneous system at  $T = 0$  using the adaptive time-dependent density matrix renormalization group algorithm<sup>24,25</sup>. In the simulation, the initial and final interaction strengths were fixed at the experimentally determined values and the quench was considered to be instantaneous, at  $t = 0$ . We found

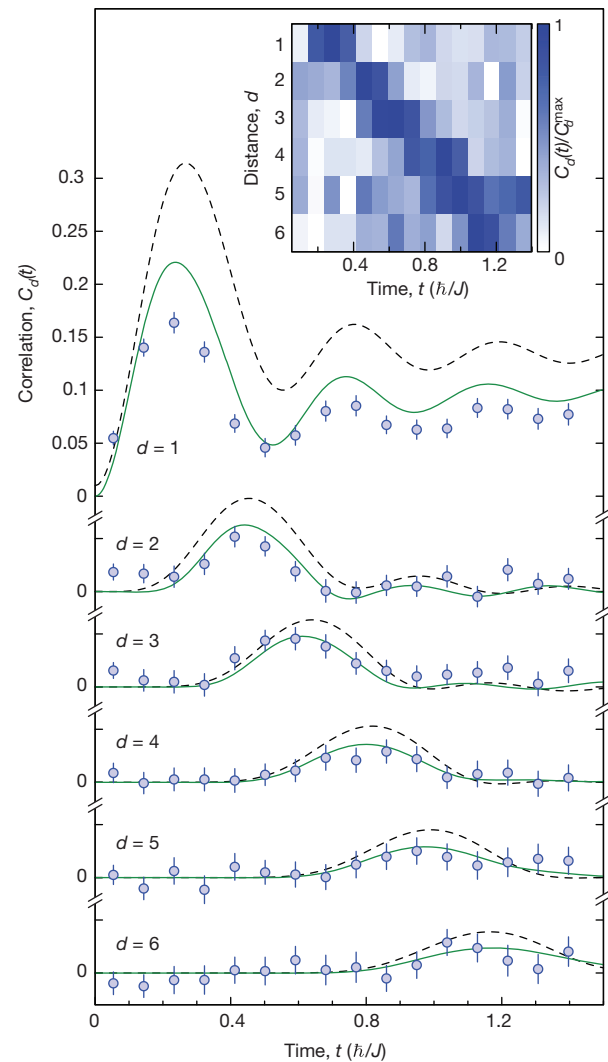


**Figure 2 | Time evolution of the two-point parity correlations.** After the quench, a positive correlation signal propagates with increasing time to larger distances. Main figure, the experimental values for a quench from  $U/J = 40$  to  $U/J = 9.0$  (open circles) are in good agreement with the corresponding numerical simulation for an infinite, homogeneous system at zero temperature (continuous green line). Our analytical model (dashed black line) also qualitatively reproduces the observed dynamics. Inset, experimental data displayed as a colour map (colour scale at right), revealing the propagation of the correlation signal with a well defined velocity. The experimental values result from the average over the central  $N$  sites of more than 1,000 chains, where  $N$  equals 80% of the length of each chain. Error bars, s.d.

remarkable agreement between the experiment and theory over all explored distances and times, despite the finite temperature and the harmonic confinement with frequency  $\nu = 68(1)$  Hz that characterize the experimental system. The observed dynamics is also qualitatively reproduced by our analytical model for  $U/J = 9.0$ . For lower values of  $U/J$ , however, the model breaks down owing to the increasing number of quasiparticles.

We extracted the propagation velocity  $v$  from the time of the correlation peak as a function of the distance  $d$  (Fig. 3a). A linear fit restricted to  $2 \leq d \leq 6$  yields  $vh/(Ja_{\text{lat}}) = 5.0(2)$ ,  $5.6(5)$  and  $5.0(2)$  for  $U/J = 5.0(2)$ ,  $7.0(3)$  and  $9.0(3)$ , respectively. The points for  $d = 1$  were excluded from the fit, as they result from the interference between propagating and bound quasiparticle pairs (see equation (1)). A comparison of the experimental velocities with those obtained from numerical simulations (Fig. 3b) shows agreement within the error bars. The measured velocities can also be compared with two limiting cases: on the one hand, they are significantly larger than the spreading

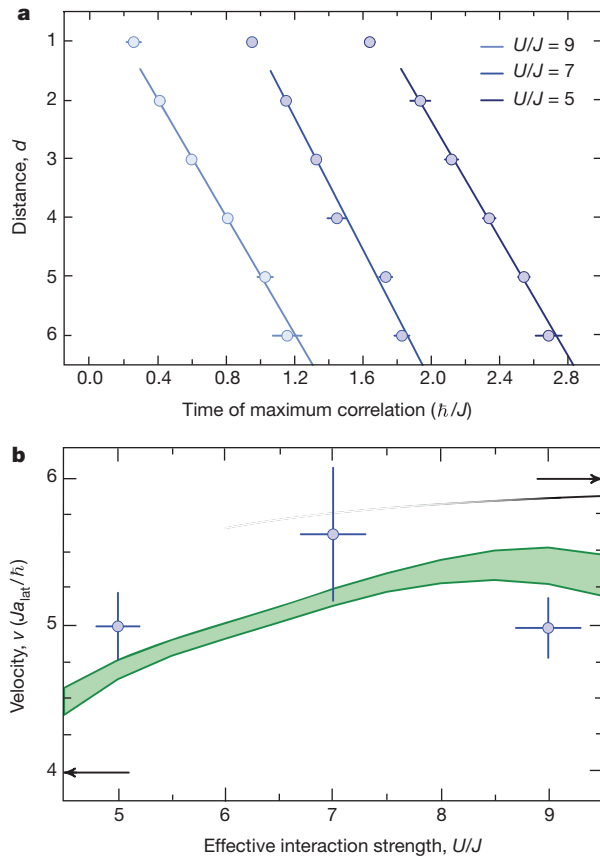


**Figure 3 | Propagation velocity.** **a**, Determination of the propagation velocity for the quenches to  $U/J = 5.0$  (open circles, dark blue),  $7.0$  (medium blue) and  $9.0$  (light blue). The time of the maximum of the correlation signal is obtained from fits to the traces  $C_d(t)$  for distances  $d = 1$  to  $6$ . Error bars, the 68% confidence interval of these fits. We then extract the propagation velocities from weighted linear fits restricted to  $2 \leq d \leq 6$  (lines). The data for  $U/J = 5.0$  and  $7.0$  have been offset horizontally for clarity. **b**, Comparison of the experimental velocities (open circles) at different interaction strengths to those obtained from numerical simulations for an infinite, homogeneous system at zero temperature (green shaded area). The shaded area and the vertical error bars denote the 68% confidence interval of the fit. The horizontal error bars represent the uncertainty due to the calibration of the lattice depth. The black line (top right) corresponds to the bound  $v_{\text{max}}$  predicted by our effective model (the fading indicates the breakdown of this model). The arrows mark the maximum velocity expected in the non-interacting case (left) and the asymptotic value derived from our model when  $U/J \rightarrow \infty$  (right).

velocity of non-interacting particles,  $v = 4 J a_{\text{lat}}/h$ , and twice the velocity of sound in the superfluid phase<sup>26</sup>; on the other hand, they remain below the maximum velocity predicted by our analytical model,  $v_{\text{max}} \approx (6 J a_{\text{lat}}/h)[1 - 16 J^2/(9 U^2)]$ , which can be interpreted as a Lieb–Robinson bound (Fig. 3b). In the limit  $U/J \rightarrow \infty$ , this bound corresponds to doublons and holons propagating with respective group velocities  $4 J a_{\text{lat}}/h$  and  $2 J a_{\text{lat}}/h$ . The higher velocity of doublons simply reflects their Bose-enhanced tunnel coupling.

We have presented the first (to our knowledge) experimental observation of an effective light cone for the spreading of correlations in an interacting quantum many-body system. Although the observed dynamics can be understood within a fermionic quasiparticle picture that is valid deep in the Mott-insulating regime, we note that our experimental data cover a region close to the critical point, for which only *ab initio* numerical simulations are available so far<sup>13</sup>. Our work opens interesting perspectives, such as revealing the entanglement carried by the quasiparticle pairs or investigating the quantum dynamics in higher dimensions, where little is known about Lieb–Robinson bounds and the scaling of entanglement. For example, the experiment can be extended to study correlation propagation in two

dimensions, where existing numerical and analytical approaches suffer from severe limitations. Furthermore, the production rate of excitations and the formation of domains when tuning the effective interaction strength slowly across the critical point can be investigated, thereby exploring a quantum analogue to the Kibble–Zurek mechanism<sup>6,27,28</sup>.

## METHODS SUMMARY

We calibrated the lattice depths by performing amplitude modulation spectroscopy of the transition between the zeroth and second Bloch band in a one-dimensional degenerate gas for the  $x$  and  $y$  axes, and in a two-dimensional degenerate gas for the  $z$  axis. We estimate the calibration uncertainty to be 1–2%.

The quench was performed by lowering the lattice depth along the  $x$  axis in an exponential way (Supplementary Information). Numerical simulations showed that the origin  $t = 0$  of the time evolution can be defined as the moment when the effective interaction strength reaches the value  $U/J \approx 17$ . We used the same phenomenological criterion to locate the moment at which the dynamics stops when raising the lattice depth to  $\sim 80 E_r$ .

We extracted the time of the maximum of the correlation signal as a function of the distance, for both the experiment and the theory, by fitting an offset-free Gaussian profile to the traces  $C_d(t)$ . For the numerical data, we filtered out frequency components above  $3 J/h$  before the fit in order to isolate the envelope of the signal. For the experimental data, we fixed the width of the Gaussian profile to the value obtained from the numerical data, keeping only the amplitude and time as free parameters.

The numerical simulations relied on matrix product states<sup>29</sup> to represent infinite homogenous systems<sup>30</sup>. Initial states were obtained using the DMRG (density matrix renormalization group) algorithm. For the time evolution, we used a second-order Suzuki–Trotter decomposition<sup>24,25</sup>. We achieved quasi-exact results on the relevant timescale  $tJ/h \approx 2$  by choosing a small enough Trotter time step ( $\sim 0.002$ ) and retaining a few thousand states.

Received 6 October; accepted 1 December 2011.

- Lieb, E. H. & Robinson, D. W. The finite group velocity of quantum spin systems. *Commun. Math. Phys.* **28**, 251–257 (1972).
- Bravyi, S., Hastings, M. B. & Verstraete, F. Lieb–Robinson bounds and the generation of correlations and topological quantum order. *Phys. Rev. Lett.* **97**, 050401 (2006).
- Calabrese, P. & Cardy, J. Time dependence of correlation functions following a quantum quench. *Phys. Rev. Lett.* **96**, 136801 (2006).
- Eisert, J. & Osborne, T. J. General entanglement scaling laws from time evolution. *Phys. Rev. Lett.* **97**, 150404 (2006).
- Nachtergaele, B., Ogata, Y. & Sims, R. Propagation of correlations in quantum lattice systems. *J. Stat. Phys.* **124**, 1–13 (2006).
- Polkovnikov, A., Sengupta, K., Silva, A. & Vengalattore, M. Nonequilibrium dynamics of closed interacting quantum systems. *Rev. Mod. Phys.* **83**, 863–883 (2011).
- Bose, S. Quantum communication through spin chain dynamics: an introductory overview. *Contemp. Phys.* **48**, 13–30 (2007).
- Hastings, M. B. Lieb–Schultz–Mattis in higher dimensions. *Phys. Rev. B* **69**, 104431 (2004).
- Nachtergaele, B. & Sims, R. Much ado about something: why Lieb–Robinson bounds are useful. Preprint at <http://arXiv.org/abs/1102.0835> (2011).
- Nachtergaele, B. & Sims, R. Lieb–Robinson bounds and the exponential clustering theorem. *Commun. Math. Phys.* **265**, 119–130 (2006).
- Hastings, M. B. & Koma, T. Spectral gap and exponential decay of correlations. *Commun. Math. Phys.* **265**, 781–804 (2006).
- Eisert, J., Cramer, M. & Plenio, M. B. Area laws for the entanglement entropy. *Rev. Mod. Phys.* **82**, 277–306 (2010).
- Läuchli, A. M. & Kollath, C. Spreading of correlations and entanglement after a quench in the one-dimensional Bose–Hubbard model. *J. Stat. Mech.* P05018 (2008).
- Nachtergaele, B., Raz, H., Schlein, B. & Sims, R. Lieb–Robinson bounds for harmonic and anharmonic lattice systems. *Commun. Math. Phys.* **286**, 1073–1098 (2009).
- Cramer, M., Serafini, A. & Eisert, J. In *Quantum Information and Many Body Quantum Systems* Vol. 8 (eds Ericsson, M. & Montangero, S.) 51–72 (Edizioni della Normale, Pisa, 2008).
- Eisert, J. & Gross, D. Supersonic quantum communication. *Phys. Rev. Lett.* **102**, 240501 (2009).
- Bloch, I., Dalibard, J. & Zwierger, W. Many-body physics with ultracold gases. *Rev. Mod. Phys.* **80**, 885–964 (2008).
- Bakr, W. S., Gillen, J. I., Peng, A., Fölling, S. & Greiner, M. A quantum gas microscope for detecting single atoms in a Hubbard-regime optical lattice. *Nature* **462**, 74–77 (2009).
- Sherson, J. F. *et al.* Single-atom resolved fluorescence imaging of an atomic Mott insulator. *Nature* **467**, 68–72 (2010).
- Fisher, M. P. A., Weichman, P. B., Grinstein, G. & Fisher, D. S. Boson localization and the superfluid-insulator transition. *Phys. Rev. B* **40**, 546–570 (1989).

21. Jaksch, D., Bruder, C., Cirac, J. I., Gardiner, C. W. & Zoller, P. Cold bosonic atoms in optical lattices. *Phys. Rev. Lett.* **81**, 3108–3111 (1998).
22. Kühner, T. D., White, S. R. & Monien, H. One-dimensional Bose–Hubbard model with nearest neighbor interaction. *Phys. Rev. B* **61**, 12474–12489 (2000).
23. Endres, M. *et al.* Observation of correlated particle-hole pairs and string order in low-dimensional Mott insulators. *Science* **334**, 200–203 (2011).
24. Daley, A. J., Kollath, C., Schollwöck, U. & Vidal, G. Time-dependent density-matrix renormalization-group using adaptive effective Hilbert spaces. *J. Stat. Mech.* P04005 (2004).
25. White, S. R. & Feiguin, A. E. Real-time evolution using the density matrix renormalization group. *Phys. Rev. Lett.* **93**, 076401 (2004).
26. Kollath, C., Schollwöck, U., von Delft, J. & Zwirger, W. One-dimensional density waves of ultracold bosons in an optical lattice. *Phys. Rev. A* **71**, 053606 (2005).
27. Kibble, T. W. B. Topology of cosmic domains and strings. *J. Phys. Math. Gen.* **9**, 1387–1398 (1976).
28. Zurek, W. H. Cosmological experiments in superfluid helium? *Nature* **317**, 505–508 (1985).
29. Schollwöck, U. The density-matrix renormalization group in the age of matrix product states. *Ann. Phys.* **326**, 96–192 (2011).
30. Vidal, G. Classical simulation of infinite-size quantum lattice systems in one spatial dimension. *Phys. Rev. Lett.* **98**, 070201 (2007).

**Supplementary Information** is linked to the online version of the paper at [www.nature.com/nature](http://www.nature.com/nature).

**Acknowledgements** We thank C. Weitenberg and J. F. Sherson for their contribution to the design and construction of the apparatus. We also thank D. Baeriswyl, T. Giamarchi, V. Gritsev and S. Huber for discussions. C.K. acknowledges previous collaboration on a related subject with A. Läuchli. We acknowledge funding by MPG, DFG, EU (NAMEQUAM, AQUIT, Marie Curie Fellowship to M.C.), JSPS (Postdoctoral Fellowship for Research Abroad to T.F.), ‘Triangle de la physique’, ANR (FAMOUS) and SNSF (under division II and MaNEP). Financial support for the computer cluster on which the calculations were performed was provided by the Fondation Ernst et Lucie Schmidheiny.

**Author Contributions** M.C. performed the experiment. P.B. performed the numerical simulations. P.B., D.P. and C.K. developed the analytical model. M.C. and P.B. carried out the data analysis. All authors contributed to designing the study, to interpreting the data and to writing the manuscript.

**Author Information** Reprints and permissions information is available at [www.nature.com/reprints](http://www.nature.com/reprints). The authors declare no competing financial interests. Readers are welcome to comment on the online version of this article at [www.nature.com/nature](http://www.nature.com/nature). Correspondence and requests for materials should be addressed to M.C. ([marc.cheneau@mpq.mpg](mailto:marc.cheneau@mpq.mpg)).